

# Implementing super-efficient FFTs in Altera FPGAs

Jérôme Leclère, Cyril Botteron, Pierre-André Farine

*Electronics and Signal Processing Laboratory (ESPLAB), École Polytechnique Fédérale de Lausanne (EPFL), Switzerland*

E-mail : jerome.leclere@epfl.ch, cyril.botteron@epfl.ch

How to cite this article : J. Leclère, C. Botteron, P.-A. Farine, "Implementing super-efficient FFTs in Altera FPGAs", EE Times Programmable Logic Designline, February 2015. Available online at [www.eetimes.com](http://www.eetimes.com).

**Abstract :** In this article, an alternative method is proposed to compute a fast Fourier transform (FFT) on Altera FPGAs. This method is using the Altera FFT intellectual property (IP) core, but it is more efficient than the direct use of the Altera FFT IP core, in the sense that the processing time or the resources can be reduced. For the FPGA user, the implementation of the proposed method is more complex than using directly the Altera FFT IP core because additional elements are required, such as a numerically controlled oscillator (NCO) or a memory, a complex multiplier, adders and scaling, but it may be worth it since the decrease in processing time or resources is significant, especially regarding the memory with large FFTs. The proposed method can also be applied to the computation of the convolution or correlation using FFTs.

## 1 Introduction

The fast Fourier transform (FFT) algorithms [1, 2] are widely used in many fields, whether for spectral analysis to detect a signal, or for computation purposes (since for example the convolution of two signals can be computed efficiently using FFTs, and the convolution is the operation performed by finite impulse response filters) [3], or for compression purposes [4] or signal enhancements [5]. In other words, FFTs are everywhere. Many applications requires the use of FPGAs, therefore, computing an FFT on an FPGA is an important problem, even in domains such as astrophysics [6]. The FPGA companies usually provide an intellectual property (IP) core to compute FFTs of length that is a power of two on their FPGA, such as Altera [7], Xilinx [8], Lattice [9] or Microsemi [10]. One could think that such IP cores are optimized for the corresponding FPGAs, however it has been found that a more efficient implementation of the Altera FFT is possible. More efficient means that the resources can be reduced for a same processing time, or that the processing time can be reduced for a moderate increase of the resources. The most surprising fact is that the alternative implementation proposed here corresponds to one step of the well-known radix-2 FFT algorithm, where two FFTs of smaller length are computed and the FFT inputs or outputs are combined.

In Section 2, we review the characteristics and parameters of the Altera FFT. In Section 3, we recall the radix-2 FFT algorithm, and show how it can be used to reduce the processing time or the resources with the Altera FFT. In Section 4, the same idea is applied for the convolution computed by FFT. Section 5 provides an application example, indicating the additional complications of the proposed implementation and the real resource usage. Finally, Section 6 concludes this paper.

## 2 Description of the Altera FFT

The implementation of an FFT algorithm on an FPGA is not an easy task. Hopefully, FPGA companies usually provide an FFT IP core. In this paper, we will concentrate on the FFT core provided by Altera, because we are working with Altera FPGAs in our different research projects. The Altera FFT [7] is highly configurable, for example we can select :

- The transform length, which must be a power of two. Currently, the minimum length is 8 points and the maximum length is 262 144 points (this is for the version 14.1 of August 2014; the maximum length may grow in the next years).
- The input/output (I/O) data flow (more details about this are provided below).

- The number of bits to quantify the input data, the output data, and the twiddle factors.
- The order of the input and of the output (natural order or bit-reversed order, see Chapter 2 of [11] for more information on this).
- Some options for the FFT engine.
- Some options for the implementation of the complex multipliers (we can use 4 multipliers and 2 adders or 3 multipliers and 5 adders, and we can implement them using digital signal processing (DSP) blocks or logic cells).
- The repartition of the memory between the different memory types.

Regarding the I/O data flow, four are available : variable streaming, streaming, buffered burst, burst. For the variable streaming and the streaming I/O data flows, the input and output data flows can be continuous, without any break between consecutive transforms. The corresponding timing diagram of an  $N$ -point FFT (shown in Fig. 1 (a)) is given in Fig. 1 (b). Between the last input sample and the first output sample of the FFT, there is a latency, denoted  $L_N$ , which depends on the transform length. Therefore, in this case, the  $P$ th FFT result is fully available after  $N + L_N + PN = (P + 1)N + L_N$  clock cycles. For the burst I/O data flow, it is possible to load a new input only when the output is completely unloaded. This means that the throughput is reduced compared to the variable streaming and streaming implementations. The buffered burst data flow is between the two previous cases. The flow cannot be continuous, but it is not required to wait for the complete unload of the output samples before loading new input samples.

Of course, the higher is the throughput, the higher are the required resources. For example, an estimate of the resources considering three I/O data flows is provided in Table 1. Playing with the engine options may lower the resources (logic, memory and DSP) for the buffered burst and burst I/O data flows, in exchange of a reduced throughput.

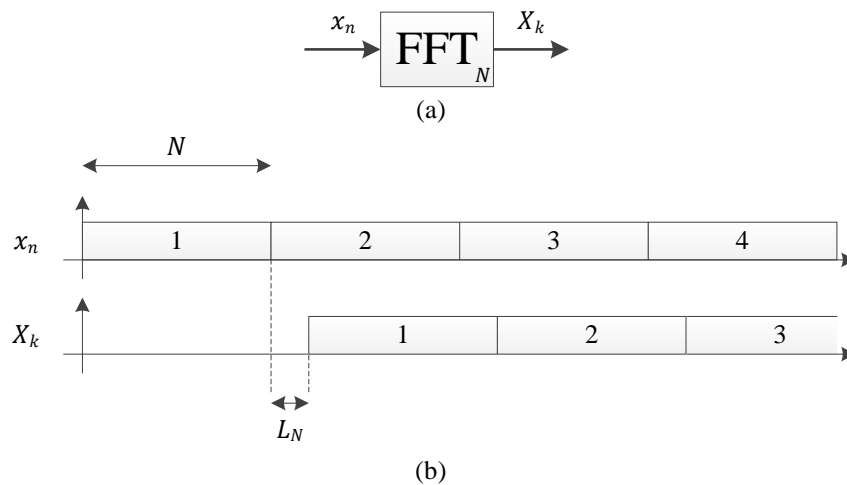


Fig. 1: (a)  $N$ -point Altera FFT, (b) corresponding timing diagram with the streaming I/O data flow (the number in the boxes identifies the sequences).

Table 1: Resources estimated with the Altera FFT IP core for an FFT of 2048 points implemented on a Cyclone V FPGA, considering 16 bits for the data and twiddle precision, and 2 FFT engines with quad output. <sup>(1)</sup>Defined as the minimum number of cycles between the start of two consecutive sequences. <sup>(2)</sup>An M10K memory contains 10 Kibit = 10 240 bits, however, the number of bits is divided by 8 instead of 10 for the conversion here due to the 16 bits resolution and the memory limitation (see Chapter 2 of [12]).

I/O data flow	Inverse of the throughput <sup>(1)</sup> (cycle)	Logic usage (logical element, LE)	Memory usage		Multipliers usage (DSP block)
			bit	M10K <sup>(2)</sup>	
Streaming	2048	5930	311 296	38	12
Buffered Burst	2304	6186	245 760	30	12
Burst	5485	5709	114 688	14	12

Due to the large number of possibilities for the FFT implementation, for the evaluation of the resources in the following sections, we will consider a Cyclone V FPGA, the streaming I/O data flow, a data and twiddle precision of 16 bits, complex multipliers implemented in DSP blocks using four real multipliers, and no logic function implemented in memory.

Under these conditions, the resources according to the FFT length are given in Table 2. It can be observed that doubling the FFT length doubles the processing time, increases slightly the logic (except for some cases), roughly doubles the memory (except for lengths lower than 512 points), and the number of DSP blocks stays the same (except between 1024 and 2048 where it doubles). Seeing this, and knowing that an FFT can be computed as two FFTs of length halved (or using time multiplexing technique, only one FFT of length halved can be used), one can imagine that these characteristics can be exploited to improve the efficiency of the implementation, which is shown in the next section.

**Table 2: Resources estimated with the Altera FFT IP core for an implementation on a Cyclone V FPGA, considering the streaming I/O data flow and 16 bits for the data and twiddle precision.**

FFT length	Inverse of the throughput (cycle)	Logic usage (LE)	Memory usage (bit)	Multipliers usage (DSP block)
64	64	3584	90 112	6
128	128	3170	90 112	6
256	256	3741	90 112	6
512	512	4135	90 112	6
1024	1024	4712	155 648	6
2048	2048	5930	311 296	12
4096	4096	6331	622 592	12
8192	8192	6080	1 245 184	12
16 384	16 384	6487	2 334 720	12
32 768	32 768	6230	4 513 492	12
65 536	65 536	6644	8 871 936	12

### 3 Efficient FFT computation on Altera FPGAs

#### 3.1 Radix-2 FFT algorithm

The discrete Fourier transform (DFT) of a sequence  $x_n$  of  $N$  points is defined as

$$X_k = \sum_{n=0}^{N-1} x_n e^{-\frac{j2\pi kn}{N}}, \quad (1)$$

with  $k = 0, 1, \dots, N-1$ . The radix-2 FFT algorithm consists in separating the input or the output in even and odd samples, and repeats the process until a certain limit [11]. Doing so once for the input, we have

$$\begin{aligned} X_k &= \sum_{n=0}^{N/2-1} x_{2n} e^{-\frac{j2\pi k(2n)}{N}} + \sum_{n=0}^{N/2-1} x_{2n+1} e^{-\frac{j2\pi k(2n+1)}{N}} \\ &= \sum_{n=0}^{N/2-1} x_{2n} e^{-\frac{j2\pi kn}{N/2}} + e^{-\frac{j2\pi k}{N}} \sum_{n=0}^{N/2-1} x_{2n+1} e^{-\frac{j2\pi kn}{N/2}}, \end{aligned} \quad (2)$$

still with  $k = 0, 1, \dots, N-1$ . The two sums does not correspond to DFTs because the range for  $k$  and  $n$  is different. The first half of  $X_k$  is obtained from Eq. (2) for  $k = 0, 1, \dots, N/2-1$ , and is

$$X_k = \sum_{n=0}^{N/2-1} x_{2n} e^{-\frac{j2\pi kn}{N/2}} + e^{-\frac{j2\pi k}{N}} \sum_{n=0}^{N/2-1} x_{2n+1} e^{-\frac{j2\pi kn}{N/2}}, \quad (3)$$

with  $k = 0, 1, \dots, N/2 - 1$  (in fact the equation is the same, only the range of  $k$  has changed). The two sums correspond to the DFT of the sequences  $x_{2n}$  and  $x_{2n+1}$ , respectively. The second half of  $X_k$  is obtained from Eq. (2) for  $k = N/2, N/2 + 1, \dots, N - 1$ , and can be expressed as

$$X_{k+N/2} = \sum_{n=0}^{N/2-1} x_{2n} e^{-\frac{j2\pi kn}{N/2}} - e^{-\frac{j2\pi k}{N}} \sum_{n=0}^{N/2-1} x_{2n+1} e^{-\frac{j2\pi kn}{N/2}}, \quad (4)$$

with  $k = 0, 1, \dots, N/2 - 1$ . The two sums are the same as for Eq. (3), therefore an FFT of  $N$  points can be computed using two FFTs of  $N/2$  points as shown in Fig. 2 (a). In the same way, by separating the output in even and odd samples, we obtain

$$\begin{aligned} X_{2k} &= \sum_{n=0}^{N/2-1} (x_n + x_{n+N/2}) e^{-\frac{j2\pi kn}{N/2}}, \\ X_{2k+1} &= \sum_{n=0}^{N/2-1} (x_n - x_{n+N/2}) e^{-\frac{j2\pi kn}{N/2}} e^{-\frac{j2\pi n}{N}}, \end{aligned} \quad (5)$$

with  $k = 0, 1, \dots, N/2 - 1$ ,  $x_n$  is the first half of the input sequence, and  $x_{n+N/2}$  is the second half. The two sums correspond to the DFT of the sequences  $x_n + x_{n+N/2}$  and  $(x_n - x_{n+N/2}) e^{-\frac{j2\pi n}{N}}$ , respectively. Therefore, an FFT of  $N$  points can also be computed using two FFTs of  $N/2$  points as shown in Fig. 2 (b).

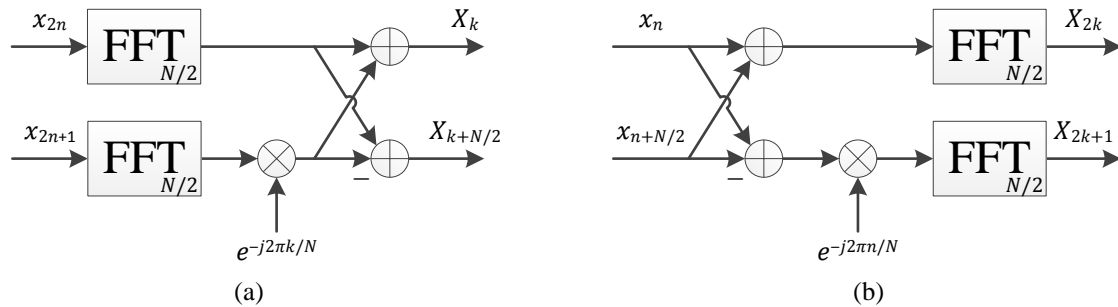


**Fig. 2 : Computation of an  $N$ -point FFT using two  $N/2$ -point FFTs, (a) where the input is separated by parity and the output is separated by section, (b) where the input is separated by section and the output is separated by parity.**

### 3.2 Application to reduce the processing time

The timing diagram corresponding to the implementation of Fig. 2(a) using Altera FFTs is depicted in Fig. 3, where  $L_{N/2}$  denotes the latency of the FFT when the transform length is  $N/2$ . In this case, the  $P$ th FFT result is fully available after  $N/2 + L_{N/2} + PN/2 = (P + 1)N/2 + L_{N/2}$  clock cycles. Therefore, compared to the direct implementation of an  $N$ -point FFT, the processing time is approximately halved (see Fig. 1 (b)). Note however that this requires having access to even and odd samples of the input sequence simultaneously.

For the evaluation of the resources, we consider  $N = 2048$ , the resources for the FFT are estimated with the Altera IP core, and the simple elements (multiplier and adder) can be easily estimated (see e.g. the models given in [13]). The complex exponential in Fig. 2 (a) can be generated either using a numerically controlled oscillator (NCO), such as the NCO IP core provided by Altera [14], or using a memory. There are different generation algorithms for the NCO IP core of Altera, and the most interesting in terms of resources is the multiplier-based one, which requires some logic, two M10K memories and two DSP blocks.

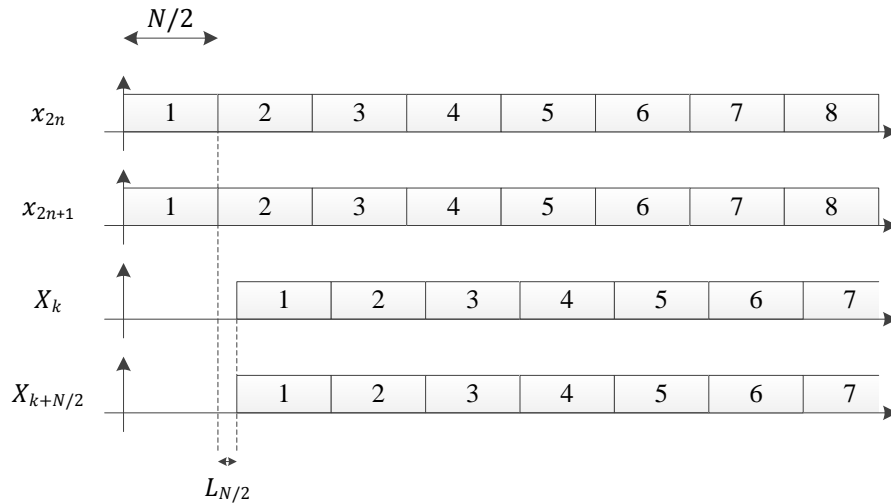


**Fig. 3: Timing diagram of the implementation of Fig. 2(a) using Altera FFTs (the number in the boxes identifies the sequences).**

If a memory is used instead, only 512 samples of 16 bits must be stored, since we need to generate half the period of a cosine and a sine, which can be obtained from only a quarter of the period of a sine wave by inverting the value and reading the memory in both directions, as shown in Fig. 4. Thus, using a dual port memory would require only one M10K, which is more interesting than using an NCO in this case, therefore this option is considered for the following. Note however, that for longer FFT lengths, the NCO becomes more interesting because it would not require more resources while the memory would need to store more samples.

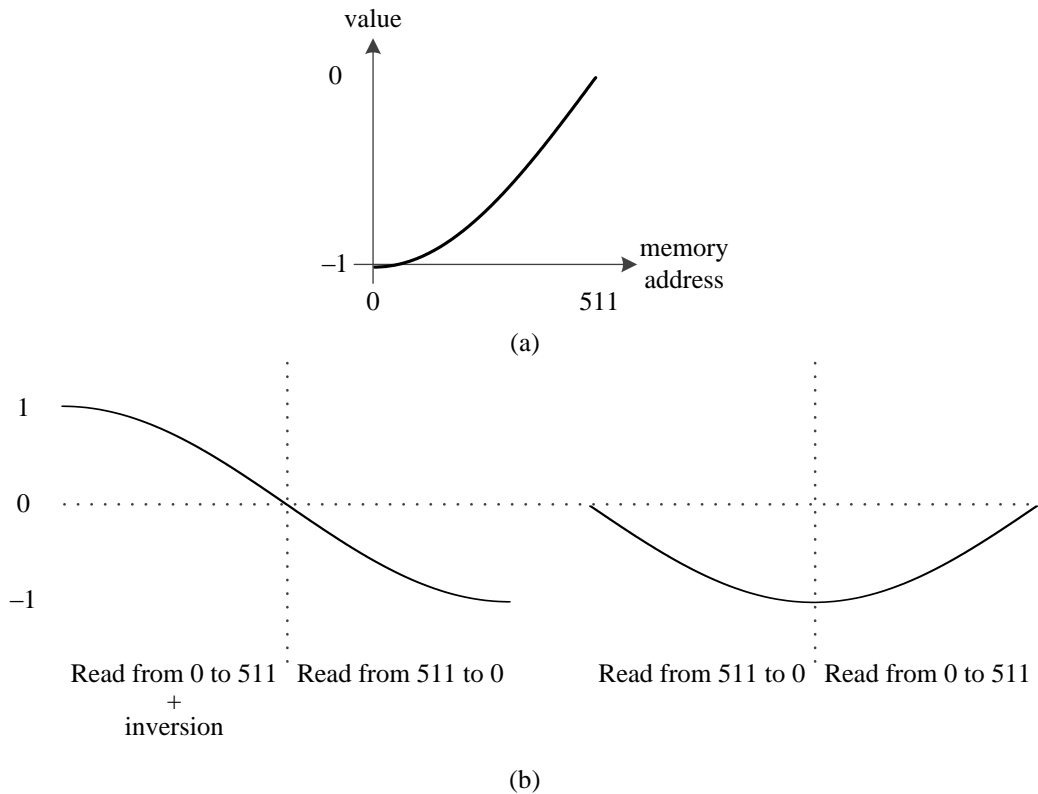


**Fig. 4: (a) Portion of a sine wave stored in the memory, (b) cosine and sine waves generated by reading the memory. The y-axis is not scaled in this illustration (e.g. using 16 bits the amplitude would be 32 767).**

**Table 3: Comparison of the resources for Fig. 2 (a) and Fig. 1 (a) using the Altera FFT with  $N = 2048$  (estimation based on Altera IP cores and models of [13]).**

Implementation	Function	Logic usage (LE)	Memory usage (M10K)	Multipliers usage (DSP block)
Fig. 2 (a)	2 FFTs (1024 points)	$2 \times 4712$	$2 \times 19$	$2 \times 6$
	Exponential generation	16	1	0
	1 Multiplier	0	0	2
	2 Adders	$2 \times 32$	0	0
	Total	9504	39	14
Fig. 1 (a)	1 FFT (2048 points)	5930	38	12
	Total	5930	38	12
Difference between Fig. 2 (a) and Fig. 1 (a)		+3574 (+60.3 %)	+1 (+2.6 %)	+2 (+16.7 %)

The summary of this basic estimation of the resources is given in Table 3, where we consider little logic for the addressing of the memory (2 buses of 8 bits). It can be seen that the implementation of Fig. 2 (a) requires more resources than the implementation of Fig. 1 (a), especially regarding the logic usage while the memory usage is almost the same. However, as shown previously, the processing time for Fig. 2 (a) is half the one for Fig. 1 (a). Since the resources are increased by a factor less than two, the implementation of Fig. 2 (a) is more efficient than the implementation of Fig. 1 (a).

### 3.3 Application to reduce the resources

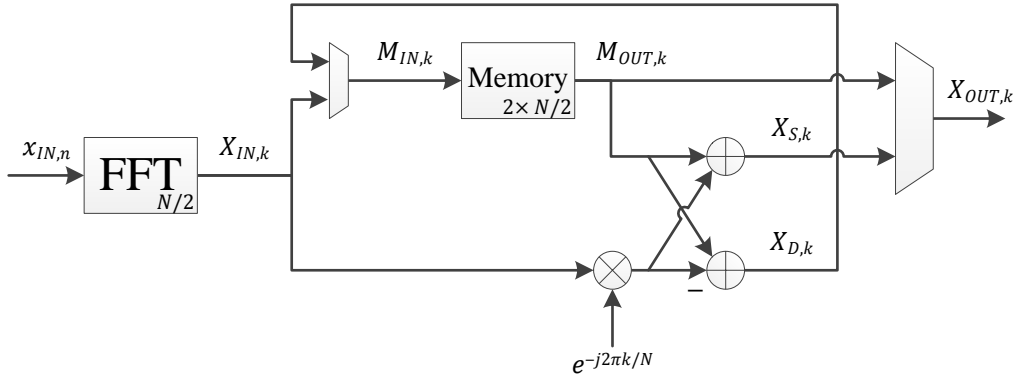
In the previous subsection, the proposed implementation was more efficient, but the resources were increased. In this subsection, we adapt it to use only one FFT, at the expense of an additional memory. The implementation is given in Fig. 5 (a), and the corresponding timing diagram is given in Fig. 5 (b). The idea is to first compute the FFT of the even samples of the sequence and to store the result in the memory. Then, the FFT of the odd samples of the sequence is computed. When the result is available, the memory is read and the first and second half of the FFT of the initial sequence is computed. The first half is outputted while the second half is stored in the memory. Once the first half is fully outputted, the memory is read and the second half is outputted. In this way, the FFT result is provided in the exact same order as the direct implementation of the FFT (Fig. 1). In this case, the  $P$ th FFT result is fully available after  $N/2 + L_{N/2} + N/2 + PN = (P + 1)N + L_{N/2}$  clock cycles, which is slightly lower than for the direct implementation because of the lower latency ( $L_{N/2} < L_N$ ).

The basic estimation of the corresponding resources is given in Table 4. For the memory, we need to store twice (because the FFT output is complex)  $1024 \times 16$  bits, which requires 4 M10K memories. It can be seen that the resources are reduced, by 19 % for the logic, 37 % for the memory, and 33 % for the DSP blocks, which is not negligible.

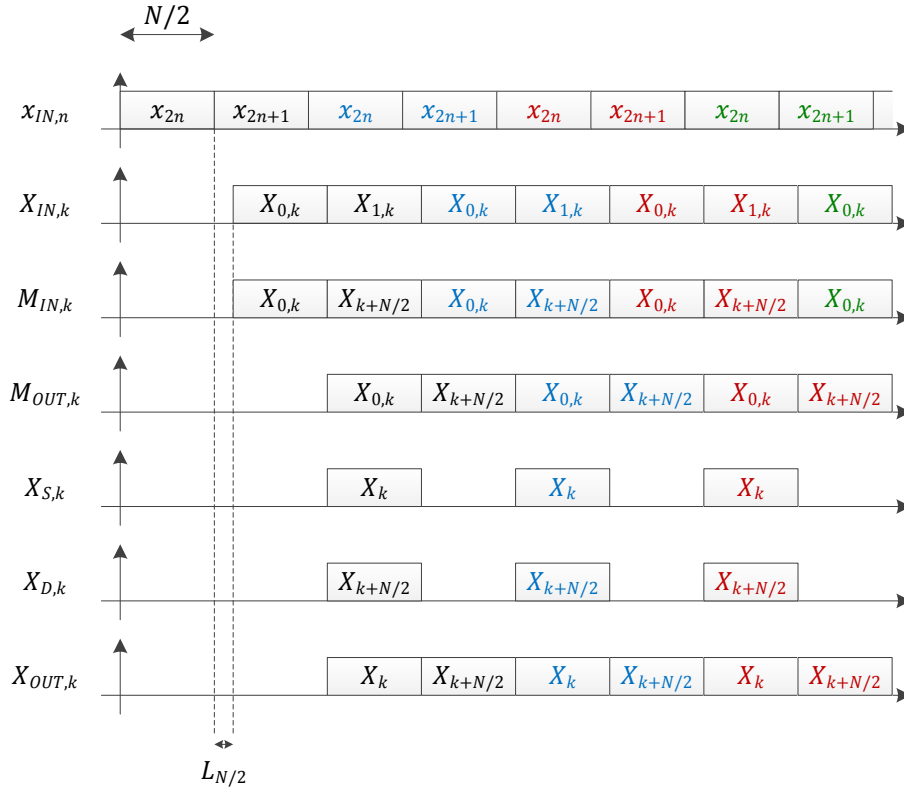
The implementation of Fig. 5 (a) assumes that the even and odd samples of the input sequence can be accessed simultaneously. If it is not the case, it is possible to add a memory to store the sequence, implying an additional latency of  $N/2$  clock cycles. In this case, 2048 samples of 16 bits should be stored, which would require 4 M10K for a real signal and 8 M10K for a complex signal. Even with this additional memory, the memory usage of the proposed implementation would be reduced by 26 % and 15 % for a real and a complex signal, respectively.

If we extrapolate to other transform lengths, the results regarding the logic and the memory would be about the same (except for lengths below 512 since the memory is not reduced anymore, as shown in Table 2). For the DSP blocks, reducing the FFT length would not reduce the number of DSP blocks (see Table 2), thus due to the additional complex multiplier, the number of DSP blocks would be slightly higher (for example if  $N > 2048$ , the proposed implementation will require 16 DSP blocks, which means an increase of 33.3 %). However, these relative values do not have the same impact because the memory usage increases linearly with the FFT length while the logic and DSP block do not, and the memory is the most used of the resources. Therefore, the absolute resource usage should be verified also, and this can represent a significant saving, especially for large FFTs. For

example, if we now consider  $N = 65\,536$ , the estimation given in Table 5 shows that if the proposed implementation has 4 additional DSP blocks (+33.3 %), the reduction of the memory resources (still of 37.1 %) means that 402 M10K blocks are saved, which is a huge amount of resources. Even if we need to store the signal before, this would require 256 M10K blocks for a complex signal ( $65\,536 \times 2 \times 16$  bits), meaning that there still would be a saving of 146 M10K blocks.



(a)



(b)

**Fig. 5: (a) Implementation of an  $N$ -point FFT using one  $N/2$ -point FFT and a memory to reduce the resources, (b) corresponding timing diagram using Altera FFTs (the colors inside the boxes identify the sequences).**

**Table 4: Comparison of the resources for Fig. 5 (a) and Fig. 1 (a) using the Altera FFT with  $N = 2048$  (estimation based on Altera IP cores and models of [13]).**

Implementation	Function	Logic usage (LE)	Memory usage (M10K)	Multipliers usage (DSP block)
Fig. 5 (a)	1 FFT (1024 points)	4712	19	6
	Exponential generation	16	1	0
	1 Multiplier	0	0	2
	2 Adders	$2 \times 32$	0	0
	1 Memory	22	4	0
	Total	4814	24	8
Fig. 1 (a)	1 FFT (2048 points)	5930	38	12
	Total	5930	38	12
Difference between Fig. 5 (a) and Fig. 1 (a)		-1116 (-18.8 %)	-14 (-36.8 %)	-4 (-33.3 %)

**Table 5: Comparison of the resources for Fig. 5 (a) and Fig. 1 (a) using the Altera FFT with  $N = 65\,536$  (estimation based on Altera IP cores and models of [13]).**

Implementation	Function	Logic usage (LE)	Memory usage (M10K)	Multipliers usage (DSP block)
Fig. 5 (a)	1 FFT (32 768 points)	6230	551	12
	NCO exponential generation	96	2	2
	1 Multiplier	0	0	2
	2 Adders	$2 \times 32$	0	0
	1 Memory	32	128	0
	Total	6422	681	16
Fig. 1 (a)	1 FFT (65 536 points)	6644	1083	12
	Total	6644	1083	12
Difference between Fig. 5 (a) and Fig. 1 (a)		-222 (-3.3 %)	-402 (-37.1 %)	+4 (+33.3 %)

## 4 Efficient convolution computation on Altera FPGAs

### 4.1 Direct implementation of the convolution

The circular convolution of two sequences  $h_n$  and  $x_n$  of  $N$  points is defined as

$$y_n = \sum_{k=0}^{N-1} h_k x_{(n-k) \bmod N}, \quad (6)$$

with  $n = 0, 1, \dots, N-1$ , and where mod denotes the modulo operation, i.e.  $(n + mN) \bmod N = n$  with  $m$  an integer. The circular convolution can also be expressed as

$$Y_k = H_k X_k, \quad (7)$$

where  $Y_k$ ,  $H_k$  and  $X_k$  are the DFTs of  $y_n$ ,  $h_n$  and  $x_n$ , respectively. So, by computing the IDFT of  $H_k X_k$  we obtain  $y_n$ . Therefore, the circular convolution can be computed efficiently as shown in Fig. 6 (a), and the corresponding timing diagram is given in Fig. 6 (b). In this case, the  $P$ th convolution result is fully available after  $N + L_N + N + L_N + PN = (P + 2)N + 2L_N$  clock cycles.



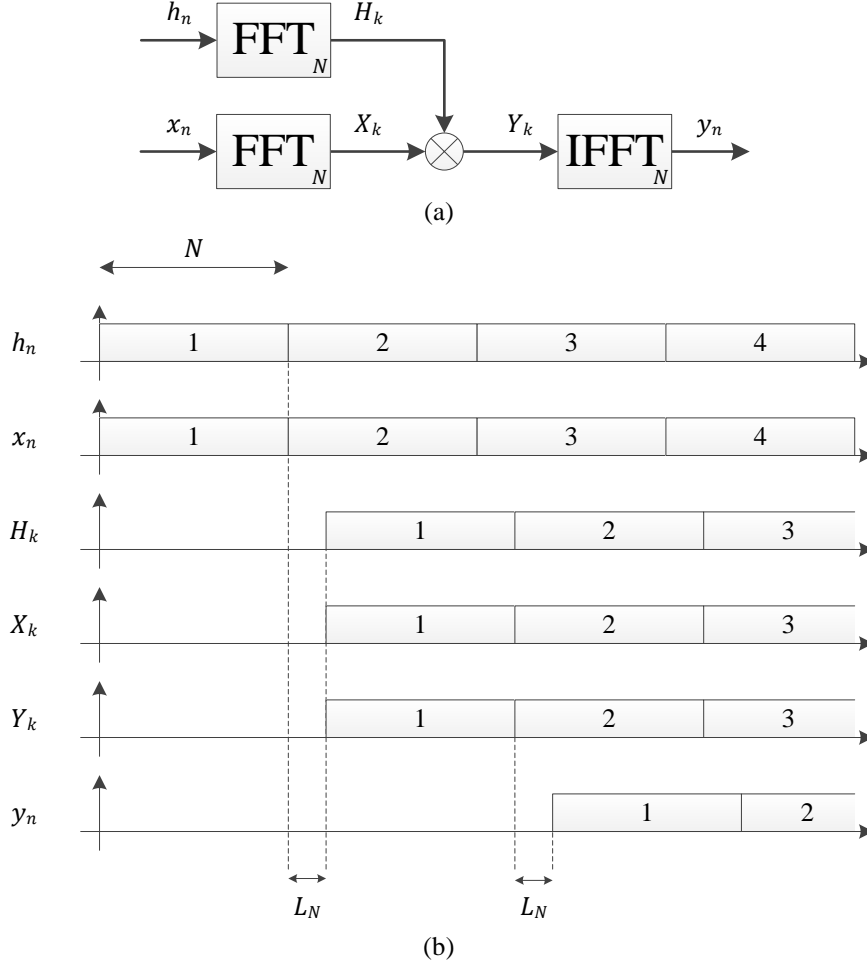


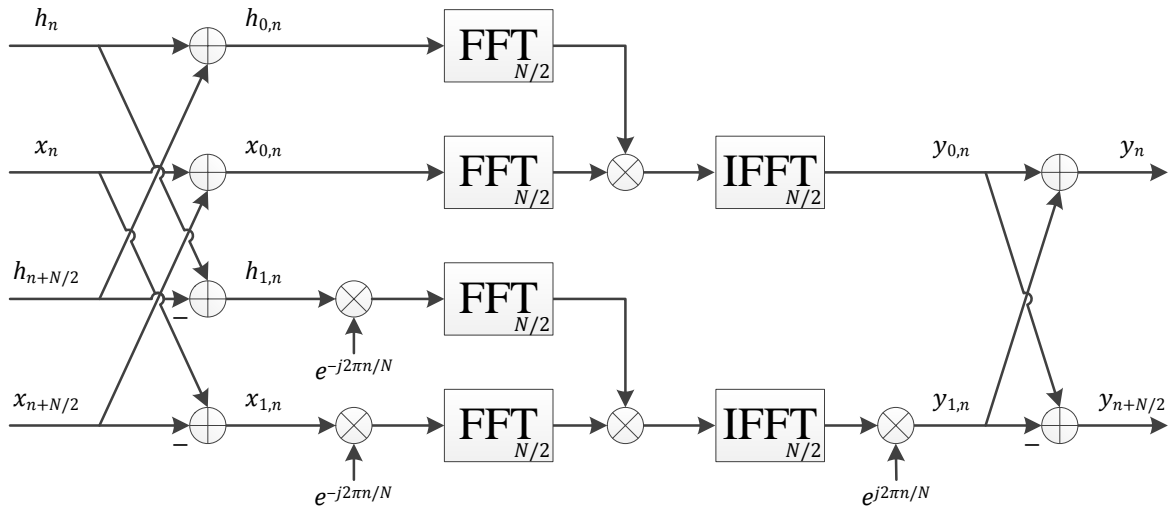
**Fig. 6: (a) Implementation of the circular convolution of two sequences of  $N$  points using FFTs, (b) corresponding timing diagram using Altera FFTs (the colors inside the boxes identify the sequences).**

#### 4.2 Application of the radix-2 FFT

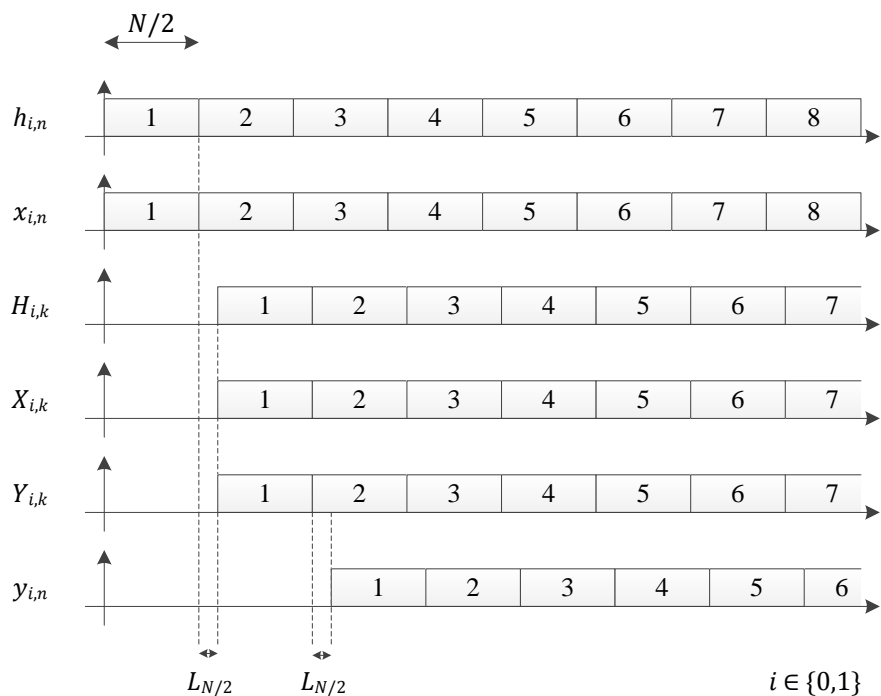
Replacing each FFT block in Fig. 6 (a) by the Fig. 2 (b), the circular convolution can be computed as shown in Fig. 7 (a), and the corresponding timing diagram is given in Fig. 7 (b). In this case, the  $P$ th convolution result is fully available after  $N/2 + L_{N/2} + N/2 + L_{N/2} + PN/2 = (P + 2)N/2 + 2L_{N/2}$  clock cycles. Therefore, compared to the direct implementation of the circular convolution (Fig. 6 (a)), the processing time is approximately halved (see Fig. 6 (b)).

For the evaluation of the resources, the same conditions as in Section 3 are considered. The basic estimation of the corresponding resources is given in Table 6. As in Section 3.2, the resources for the proposed implementation are increased by a factor less than two while the processing time is halved. Therefore, the implementation of Fig. 7 (a) is more efficient than the implementation of Fig. 6 (a). Note that moreover, slightly different implementations than Fig. 7 (a), using four multipliers instead of five, are also possible (see Chapter 4 of [15]).

The same principle can be applied to reduce the resources of the convolution, by using three  $N/2$ -point FFTs and an additional memory, and it can be verified that for the same processing time, the resources can be reduced (the reduction is even slightly higher than for the computation of an FFT shown in Section 0, see Chapter 4 of [15]).



(a)



(b)

**Fig. 7: (a) Implementation of a circular convolution of  $N$  points using  $N/2$ -point FFTs, where the inputs and the output are separated by section, (b) corresponding timing diagram using Altera FFTs (the colors inside the boxes identify the sequences).**

**Table 6: Comparison of the resources for Fig. 7 (a) and Fig. 6 (a) using the Altera FFT with  $N = 2048$  (estimation based on Altera IP cores and models of [13]).**

Implementation	Function	Logic usage (LE)	Memory usage (M10K)	Multipliers usage (DSP block)
Fig. 7 (a)	6 FFTs (1024 points)	$6 \times 4712$	$6 \times 19$	$6 \times 6$
	Exponentials generation	32	2	0
	5 Multipliers	0	0	$5 \times 2$
	6 Adders	$6 \times 32$	0	0
	Total	28 496	116	46
Fig. 6 (a)	3 FFTs (2048 points)	$3 \times 5930$	$3 \times 38$	$3 \times 12$
	1 Multiplier	0	0	2
	Total	17 790	114	38
Difference between Fig. 7 (a) and Fig. 6 (a)		+10 706 (+60.2 %)	+2 (+1.8 %)	+8 (+21.1 %)

## 5 Application example

In the previous sections, the estimation of the resources was based on estimates from the Altera IP cores and from models. To validate the previous results, the direct implementation of the Altera FFT (Fig. 1 (a)) and the proposed implementation of the Altera FFT (Fig. 2 (a)) have been implemented into a Cyclone V FPGA, in order to measure the resources after the place and route operation using the Quartus II software. The two implementations (in fact three because the proposed one has been implemented with an NCO and with a memory for the complex exponential generation), and validation by ModelSim and Matlab are available at <https://documents.epfl.ch/groups/e/es/esplab-unit/www/AlteraFFT/>.

### 5.1 Real implementation

The real implementation of the proposed method is slightly more complex than the schematic depicted in Fig. 2 (a), and is shown in Fig. 8, where the numbers represent the resolution of the signals in bit.

Regarding the memory, as indicated previously, only a quarter of a sine wave is stored. Therefore, little logic is needed to obtain the cosine and sine wave wanted. Then, the sine wave stored in the memory has an amplitude of 32 767 (since 16 bits allow a value between  $-32\,768$  and  $32\,767$ ), while the theoretical amplitude of the complex exponential is 1. Therefore, the output of the FFT of  $x_{2n}$  should also be multiplied by 32 767. This, however, can be approximated by a multiplication by 32 768, which is much easier to implement since it simply corresponds to a shift of 15 bits to the left of the signal. Therefore, this does not add resources.

With the streaming, buffered burst and burst data I/O data flows, the FFT outputs a signal and an exponent because a block-floating-point scaling is performed inside the FFT [7], and the actual FFT output can be computed as  $FFT_{output} \times 2^{-exponent}$ . Even if the even and odd samples of the input signal have the same characteristics (such as mean and variance), the exponent provided by the two FFTs can be different (typically they differ at most by 1), and therefore a scaling must be performed before adding/subtracting the signals. However, this scaling is not overly complex and does not add a lot of logic resources.

With these additional operations, the output signal has a resolution of 34 bits instead of 16 bits. The impact of this depends on the process implemented after the FFT, storing it would have a big impact, while detecting a maximum on the FFT output would have a small impact. Also, a rounding to 16 bits could be performed, at the expense of a slight reduction in the accuracy, as shown in the last plot of Fig. 9.

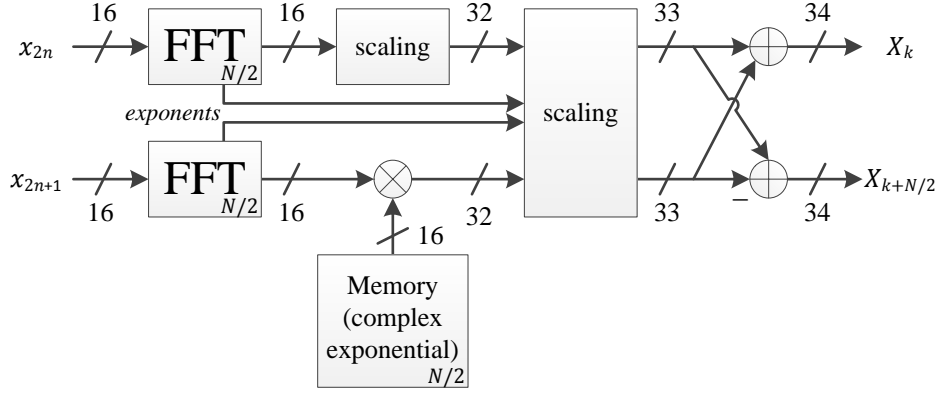


**Fig. 8 : Actual implementation of Fig. 2 (a).**

### 5.2 Performance evaluation

For testing the implementations, a memory is used to store and generate 20 480 samples of  $x_n$ , which allows the computation of 10 FFTs. For the direct implementation, the FFT latency is of 1402 clock cycles, and the time to get the 10 FFTs is 23 930 clock cycles, whereas for the proposed implementation, the FFT latency is 1084 clock cycles, and the 10 FFTs are obtained after 12 348 clock cycles. The processing time is thus divided by about 1.94 (because the length of the 10 sequences is divided by two but the FFT latency is not divided by two), as expected. The resources after the place and route operation are given in Table 7, where the Top function includes the adders, the scaling and the control signals (note that the unit for the logic is now adaptive logic module (ALM), with the approximation 1 ALM = 2.5 LEs). Comparing these values with Table 3, the performances are close to those expected, being better regarding the logic.

For checking the accuracy of the implementations, the input signal has been generated as a cosine with an additive white Gaussian noise, i.e.  $x_n = \cos(2\pi fn/f_s) + \eta(n)$ , with  $f = 200$  kHz,  $f_s = 2.048$  MHz, where  $\eta$  follows a normalized Gaussian distribution (mean of zero, variance of one). A normalization factor is also applied before and after the FFT to use the full resolution (16 bits here), because the error of the Altera FFT is higher if the most significant bits are not used. Looking at the output of the FFT, where the real part is shown in Fig. 9, it can be seen that the proposed implementation (Fig. 8) has a slightly lower error than the direct implementation (Fig. 1 (a)) of the Altera FFT if there is no rounding. If the output of the proposed implementation is rounded to 16 bits (by taking the 16 most significant bits, thus in fact it is a floor operation), the error becomes higher, but still clearly reasonable.

**Table 7: Comparison of the resources for Fig. 8 and Fig. 1 (a) using the Altera FFT with  $N = 2048$  (resources given by the Quartus II software after place and route).**

Implementation	Function	Logic usage (ALM)	Memory usage (M10K)	Multipliers usage (DSP block)
Fig. 8	Top	553	0	0
	FFT 1 (1024 points)	1578.3	20	6
	FFT 2 (1024 points)	1572.5	20	6
	Exponential generation memory	0	1	0
	1 Multiplier	0	0	2
	Total	3703.8	41	14
Fig. 1 (a)	Top	292.3	0	0
	FFT (2048 points)	2345.8	38	12
	Total	2638.1	38	12
Difference between Fig. 8 and Fig. 1 (a)		+1066.7 (+40.4 %)	+3 (+7.9 %)	+2 (+16.7 %)

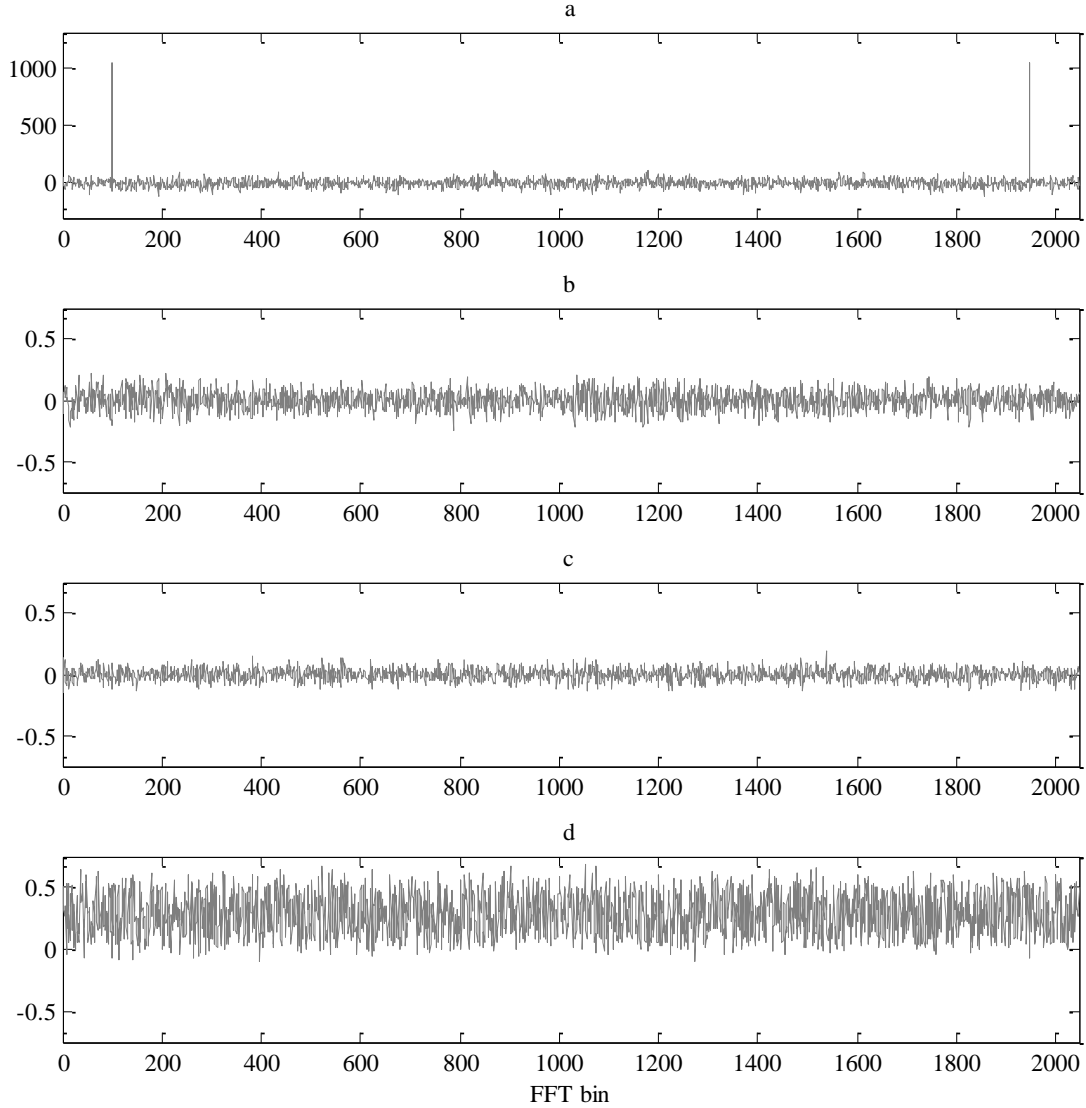


**Fig. 9 :** For the signal considered, (a) Output of the Matlab FFT, (b) Difference between the outputs of the Matlab FFT and of the Altera FFT, (c) Difference between the outputs of the Matlab FFT and of the proposed implementation using the Altera FFT (Fig. 8), (d) Difference between the outputs of the Matlab FFT and of the proposed implementation using the Altera FFT (Fig. 8) rounding the output to 16 bits. Only the real part is shown.

## 6 Conclusions

In this paper, we have shown a relatively simple way to compute an FFT on Altera FPGAs using the Altera FFT IP core providing with a better efficiency than the direct implementation of one Altera FFT. This means that it is possible to have the same processing time and use fewer resources, or that it is possible to reduce the processing for a moderate increase of the resources. The method used here is in fact one step of the radix-2 FFT, therefore the improvement may seem surprising. The method is also interesting for the convolution or correlation computed by FFT.

The potential improvement can be estimated easily with the IP cores tools, and an application example with a measure of the resources after place and route has validated the estimation. It has been shown for example that it is possible to halve the processing time for an increase of 40 %, 8 % and 17 % of the logic, memory and DSP resources, respectively. Potentially, for a same processing time, it is possible to reduce the resources by 19 %, 37 % and 33 % for the logic, memory and DSP, respectively. However, these relative values do not have the same impact because the memory usage increases linearly with the FFT length while the logic and DSP block do not, and the memory is the most used of the resources. Therefore, the absolute resource usage should be verified also, and this can represent a significant saving, especially for large FFTs. For example, with the proposed method, a streaming FFT of 65 536 points using 16 bits can be implemented with 4 additional DSP blocks

(+33 %) but with about 400 M10K blocks less (−37 %), for the same processing time, which is clearly interesting because this represents a huge amount of resources. Finally, the actual improvement will depend on the I/O data flow, the parameters and the FPGA selected.

## 7 References

- 1 L. Brigham, “The fast Fourier transform and its applications”, Prentice Hall, 1988.
- 2 P. Duhamel, M. Vetterli, “Fast Fourier transforms: A tutorial review and a state of the art”, *Signal Processing*, vol. 19, no. 4, pp 259–299, 1990.
- 3 H.J. Nussbaumer, “Fast Fourier transform and convolution algorithms”, Springer, 2nd edition, 1982.
- 4 S.W. Smith, “Digital signal processing: a practical guide for engineers and scientists”, Newnes, 2002.
- 5 A.E. Zonst, “Understanding FFT applications”, Citrus Press, 2nd edition, 2003.
- 6 T.S. Czajkowski, C.J. Comis, M. Kawokgy, “Fast Fourier transform implementation for high speed astrophysics applications on FPGAs”, VLSI Systems Project Report, June 2004.
- 7 Altera, “FFT MegaCore Function – User Guide”, August 2014.
- 8 Xilinx, “LogiCORE IP Fast Fourier Transform – Product Guide”, April 2014.
- 9 Lattice, “FFT Compiler IP Core User’s Guide”, August 2011.
- 10 Microsemi, “Core FFT – Handbook”, September 2013.
- 11 R.G. Lyons, “Understanding digital signal processing”, Prentice Hall, 4th edition, 2010.
- 12 Altera, “Cyclone V Device Handbook, Volume 1”, July 2014.
- 13 J. Leclère, C. Botteron, P.-A. Farine, “Comparison Framework of FPGA-Based GNSS Signals Acquisition Architectures”, *IEEE Transactions on Aerospace and Electronic Systems*, vol. 49, no. 3, pp 1497–1518, 2013.
- 14 Altera, “NCO MegaCore Function – User Guide”, August 2014.
- 15 J. Leclère, “Resource-efficient parallel acquisition architectures for modernized GNSS signals”, PhD thesis, EPFL, 2014.

## Author biographies

Dr. Jérôme Leclère received a master and an engineering degree in Electronics and Signal Processing from ENSEEIHT, Toulouse, France, in 2008, and his Ph.D. in the GNSS field from EPFL, Switzerland, in 2014. He focused his researches in the reduction of the complexity of the acquisition of GNSS signals, with application to hardware receivers, especially using FPGAs. He developed an FPGA-based high sensitivity assisted GPS L1 C/A receiver, and participated to the design of several FPGA receivers, for space applications (L1 C/A) and for GNSS reflectometry (L1/E1).

Dr. Cyril Botteron is leading, managing, and coaching the research and project activities of the Global Navigation Satellite System and Ultra-Wideband and mm-wave groups at École Polytechnique Fédérale de Lausanne (EPFL). He is the author or co-author of 5 patents and over 100 publications in major journals and conferences in the fields of wireless positioning systems, GNSS-based navigation and sensing, ultra-low-power radio frequency communications and integrated circuits design, and baseband analog and digital signal processing.

Prof. Pierre-André Farine is professor in electronics and signal processing at EPFL, and is head of the electronics and signal processing laboratory. He received the M.Sc. and Ph.D. degrees in Micro technology from the University of Neuchâtel, Switzerland, in 1978 and 1984, respectively. He is active in the study and implementation of low-power solutions for applications covering wireless telecommunications, ultra-wideband, global navigation satellite systems, and video and audio processing. He is the author or co-author of more than 120 publications in conference and technical journals and 50 patent families (more than 270 patents).